nanomaterials

MDPI

Review

Interaction Mechanisms and Application of Ozone Micro/Nanobubbles and Nanoparticles: A Review and Perspective

Wei Xiao [1,2,*], He Zhang [1], Xiaohuan Wang [3], Biao Wang [4], Tao Long [1], Sha Deng [1] and Wei Yang [1]

[1] School of Resources Engineering, Xi'an University of Architecture and Technology, Xi'an 710055, China; hezhangxauat@163.com (H.Z.); longtao@xauat.edu.cn (T.L.); dengsha@xauat.edu.cn (S.D.); yangweixauat@126.com (W.Y.)
[2] Western Mining Company Limited, Xining 810002, China
[3] School of Economics and Technology, Anhui Agricultural University, Hefei 230036, China; wxh17733351152@163.com
[4] Anhui Hengyu Environmental Protection Equipment Manufacturing Company Limited, Fuyang 230036, China; wb1056669818@163.com
* Correspondence: wei.xiao@xauat.edu.cn; Tel.: +86-029-8220-3408

Abstract: Ozone micro/nanobubbles with catalytic processes are widely used in the treatment of refractory organic wastewater. Micro/nanobubble technology overcomes the limitations of ozone mass transfer and ozone utilization in the application of ozone oxidation, and effectively improves the oxidation efficiency of ozone. The presence of micro/nanobubbles keeps the catalyst particles in a dynamic discrete state, which effectively increases the contact frequency between the catalyst and refractory organic matter and greatly improves the mineralization efficiency of refractory organic matter. This paper expounds on the characteristics and advantages of micro/nanobubble technology and summarizes the synergistic mechanism of microbubble nanoparticles and the mechanism of catalyst ozone micro/nanobubble systems in the treatment of refractory organics. An interaction mechanism of nanoparticles and ozone microbubbles is suggested, and the proposed theories on ozone microbubble systems are discussed with suggestions for future studies on systems of nanoparticles and ozone microbubbles.

Keywords: ozone micro/nanobubbles; titanium dioxide; phenolic pollutants; photocatalysis; hydroxyl radical

Citation: Xiao, W.; Zhang, H.; Wang, X.; Wang, B.; Long, T.; Deng, S.; Yang, W. Interaction Mechanisms and Application of Ozone Micro/Nanobubbles and Nanoparticles: A Review and Perspective. *Nanomaterials* **2022**, *12*, 1958. https://doi.org/10.3390/nano12121958

Academic Editor: Marco Stoller

Received: 6 May 2022
Accepted: 2 June 2022
Published: 7 June 2022

1. Introduction

In recent years, advanced oxidation methods with green and efficient characteristics have attracted the attention of researchers in the field of water treatment [1,2]. Advanced oxidation methods in the process of water treatment, through the input of light energy, electrical energy and other external energy and O_3, H_2O_2 and other substances [3], via a series of physical processes and chemical reactions, generate hydroxyl radicals (·OH) and peroxyradical ($O_2\cdot^-$) active radicals with strong oxidability [4], and the generated hydroxyl radicals can react quickly with electron sites that are rich in organic matter in water, which triggers complex free radical chain reactions, thereby resulting in the degradation and removal of organic matter [5].

As a kind of advanced oxidation technology, ozone catalytic oxidation technology has the characteristics of high oxidation efficiency and no secondary pollution, which can degrade the refractory organic matter in waste and has been widely used in the field of water treatment [6–9]. However, the low ozone utilization rate and poor mass transfer efficiency in the ozone catalytic oxidation process need to be overcome. Researchers' strategies for improving ozone catalytic oxidation technology can be divided into two categories: catalyst modification [10,11] and the combination of ozone catalytic oxidation

with other water treatment processes [12–14]. TiO_2 nanoparticles (TNPs) have higher catalytic efficiency than plate materials due to their fineness, surface effect and small size effect [15,16].

Micro/nanobubble technology overcomes the limitations of traditional ozone catalytic oxidation technology and effectively improves the utilization rate and mass transfer rate of ozone [17,18]. Micro/nanobubbles can not only accelerate the decomposition of ozone's hydroxyl radicals, but also release many hydroxyl radicals, which greatly improves the mineralization efficiency of refractory organic compounds [19–21]. At the same time, the presence of micro/nanobubbles can also keep the catalyst in a dynamic discrete state, which effectively increases the contact frequency between the catalyst and refractory organic matter and contributes to improving the mineralization efficiency of refractory organic matter [12,22,23].

2. Research Status of Phenolic Pollutants

2.1. Sources and Hazards of Phenolic Organic Compounds

Phenol and its derivatives are common raw materials and intermediates in China's industrial production. They are widely used in printing and dyeing [24,25], the chemical industry [26,27] and other applications. Phenolic pollutants are inevitably present in wastewater that is discharged from petrochemical, coking, liquefaction and other industrial production sources [28–32] and have large impacts on human health and the surrounding water environment. According to the national environmental statistics bulletin [33], the discharge of wastewater in China in 2019 was as high as 567.1 tons, of which the discharge of industrial source wastewater that contained volatile phenol was 147.1 tons, which accounted for 25.94% of the total discharge of wastewater. Therefore, the removal of phenolic pollutants from wastewater is the top priority in water environmental treatment.

As the simplest and most basic cyclic hydrocarbon pollutant among phenolic pollutants, phenol is characterized by strong toxicity, good water solubility and difficult natural degradation in environmental water. It is a typical refractory organic pollutant. Phenol and other phenolic pollutants are highly toxic. Phenol in wastewater not only causes damage to the human nervous system, but also leads to headache, anemia and even acute poisoning, which threatens the growth of fish and microorganisms in water [34]. If the content of phenol in the water reaches 5 mg/L, the fish will die of poisoning. At the same time, phenol-containing wastewater also has a severe impact on the aquatic environment. For example, wastewater that contains a high concentration of phenol cannot be used for farmland irrigation; otherwise, it will lead to the reduction and even apoptosis of agricultural products [35]. In view of the toxicity of phenol and other phenolic pollutants, many countries prioritize the prevention and control of water pollution [36]. China's pollutant discharge standard for urban sewage treatment plants (GB18918-2002) clearly stipulates that the maximum allowable emission concentration (daily average value) of volatile phenol in the discharge of water pollutants from urban sewage treatment plants should not be higher than 0.5 mg/L [37], and the discharge of untreated phenolic wastewater is prohibited.

2.2. Treatment of Phenolic Pollutants

With the vigorous development of the coal chemical industry, the petrochemical industry and other industries, the demand for phenolic organics has also increased, and the discharge of phenolic pollutants has brought a large load to the water supply environment. In the process of phenol degradation, various active free radicals [34] are often produced by photocatalysts in the production of intermediate products, such as catechol, hydroquinone and p-benzoquinone, which are finally degraded and mineralized. Efficient degradation and even mineralization of phenol and other phenolic pollutants in wastewater has become a research hotspot in the field of water treatment.

At present, the treatment methods of phenol containing wastewater mainly include physicochemical methods, biochemical methods and advanced oxidation:

(1) Physicochemical methods separate insoluble pollutants in water through mass transfer between different media. They have a good treatment effect on wastewater containing high concentrations of phenol. Because physicochemical methods do not change the chemical properties of the substances in the treatment process, they have the characteristics of simple operation, high system stability and high removal rate [14].
(2) Biochemical methods remove phenolic substances from sewage by domesticating microorganisms with the ability to degrade phenolic pollutants. By domesticating and optimizing the microbial population, using phenolic substances as carbon sources and energy and taking the intake of phenolic substances that are required for their own growth as the degradation mode for degrading phenolic pollutants, biochemical methods provide the advantages of maintaining efficient dominant strains, high treatment efficiency and harmless wastewater treatment [38].
(3) Advanced oxidation methods use oxidation technology with ·OH as the main oxidant. They produce ·OH with strong oxidation using light, electricity or catalysts, which can convert phenolic organics into low-toxicity or nontoxic small molecule organics without selectivity [39]. Advanced oxidation methods have the advantages of a fast reaction rate, complete degradation, no secondary pollution and a wide application range. They are a more effective technology for the treatment of phenolic pollutants [40]. Representative processes include the Fenton oxidation method, electrocatalytic oxidation methods and ozone catalytic oxidation method. Ozone catalytic oxidation methods can be divided into homogeneous catalysis and heterogeneous catalysis according to the type of catalyst. The former decomposes ozone through transition metal ions, and the latter promotes ozone decomposition through solid catalysts [8].

3. Ozone Catalytic Oxidation Process

Using the ozone process alone, the utilization rate of ozone is not high, and the mineralization rate of organic matter is low. The combined application of the ozone process and other technologies can achieve low consumption and high efficiency and completely mineralize refractory organic matter. Ozone oxidation with a catalyst is called catalytic ozone oxidation. Catalytic ozone oxidation uses a catalyst to catalyze ozone decomposition to produce ·OH, $\cdot O_2^-$ and other active oxygen free radicals with strong oxygen free radicals to oxidize and degrade organic substances. According to the catalyst type and structure, ozone catalytic oxidation can be divided into homogeneous catalytic oxidation and heterogeneous catalytic oxidation [8].

Many semiconductor materials with photocatalytic properties, such as TiO_2, ZnO, ZnS, WO_3 and SnO_2, are used as photocatalysts [41], but ZnO and CdS are unstable under light, and Zn^{2+} and Cd^{2+} are corrosive, which will result in secondary pollution to the environment. As a photocatalyst, TiO_2 has become a research hotspot in the field of photocatalytic technology for water treatment because of its nontoxic and harmless nature, strong chemical stability and high catalytic efficiency [42].

3.1. Basic Properties of TiO_2 Nanoparticle Photocatalysts

Due to the refinement of particles, TiO_2 nanoparticles (TNPs) have surface effects and small-size effects that plate materials do not have [43], which makes the catalytic efficiency of TNP photocatalysts better. TiO_2 has the following advantages:

(1) High electrocatalytic efficiency. TiO_2 undergoes an electron transition under light conditions, and the electron hole with strong oxidation that is formed by the electron in the conduction band adsorbs and oxidizes the organic matter and solvent on the semiconductor surface [44].
(2) Excellent chemical stability. TiO_2 has strong acid and alkali resistance and photochemical corrosion resistance.
(3) Energy saving and low cost. The band gap of TiO_2 is 3.0–3.2 eV, and the ultraviolet part of natural energy sunlight can be used as the light source.

(4) The reaction conditions are mild, and the final products are TiO_2, H_2O and other harmless substances, which do not produce secondary pollution, and have high potential for energy conservation, conservation and environmental protection.

When TiO_2 is irradiated by light whose energy is equal to or greater than the band gap width, an electron transition occurs, and the electron (e^-) on the valence surface excites and transitions to the conduction band [45]. Then, an electron hole pair ($e - h^+$) is generated on the valence band, which directly oxidizes and reduces the pollutants that are adsorbed on the surface, or oxidizes the hydroxyl groups (OH^-) on the adsorption surface into hydroxyl radicals (·OH) with strong oxidation and then oxidizes and degrades the organic matter into H_2O, CO_2 and other harmless small molecular products [46].

The main mechanism of the photocatalytic reaction is the oxidation of high activity and highly oxidizing ·OH, and the photocatalytic process generates a series of strongly oxidizing free radicals through a free radical chain reaction to realize the mineralization of organic pollutants.

As illustrated in Figure 1, a series of TiO_2 reaction processes in photocatalysis can be expressed by the following reaction formulae:

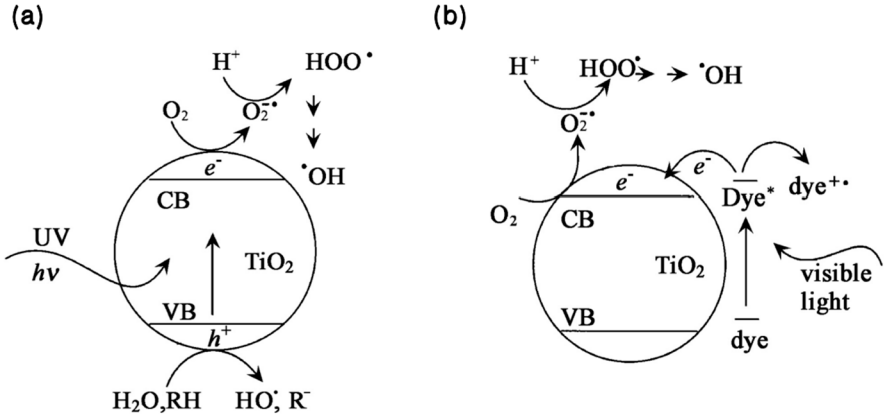

Figure 1. Reaction mechanism diagram of TiO_2 photocatalytic oxidation under UV (**a**) and visible light (**b**) [47]. Reprinted with permission from Ref. [47].

Photoinduced excitation:

$$TiO_2 + h\upsilon \rightarrow TiO_2 + e^- + h^+$$

Production of ·OH by holes under the action of an electric field:

$$TiO_2(h^+) + H_2O \rightarrow TiO_2 + H^+ + OH^-$$

$$TiO_2(h^+) + OH^- \rightarrow TiO_2 + \cdot OH$$

Capture of electrons by oxygen and production of ·OH:

$$TiO_2(e^-) + O_2 \rightarrow TiO_2 + \cdot O_2^-$$

$$H_2O + h^+ \rightarrow \cdot OH + H^+$$

$$\cdot O_2^- + H^+ \rightarrow HOO\cdot$$

$$2HOO\cdot \rightarrow H_2O_2 + O_2$$

$$H_2O_2 + e^- \rightarrow \cdot OH + OH^-$$

$$H_2O_2 + \cdot O_2^- \rightarrow \cdot OH + OH^- + O_2$$

Oxidization and degradation of the organic matter:

$$\cdot OH + O_2 + \text{Organic} \rightarrow H_2O + CO_2 + \text{etc.}$$

3.2. Application of TiO_2 Catalyzed Oxidation

The use of TiO_2 for the photocatalytic degradation of phenolic pollutants has been studied and reported by many scholars. To eliminate the TiO_2 bottleneck for the further practical application of photocatalysts, researchers have made many efforts to broaden the light response range and improve the quantum conversion efficiency, and a variety of TiO_2 modification methods [48–50] have been put forward to effectively improve the efficiency TiO_2 in the photocatalytic degradation of phenolic pollutants [51].

(1) Nonmetallic doping modification. Nonmetallic materials are widely available and inexpensive, and nonmetallic ions are doped into the lattice of TiO_2 to replace the oxygen vacancies of TiO_2 [52], which can not only reduce the band gap of TiO_2 nanoparticles and broaden the visible light response range [53–55], but also effectively inhibit the recombination of photocarriers [56] and improve their photocatalytic performance.

(2) Surface noble metal deposition modification. When a precious metal is loaded on the surface of TiO_2, the electrons transfer due to the Fermi energy level [57]: TiO_2 particles with higher Fermi energy levels will lose electrons and thus gain positive charge, while noble metals will gain negative charge because of electron capture, which makes organic matter more easily photooxidized to secondary holes [58–60]. The recombination of holes and photogenerated electrons in the TiO_2 catalyst can be effectively inhibited [61], thus the transfer efficiency of photogenerated electrons and photocatalytic performance of the TiO_2 catalyst can be improved.

(3) Oxide composite semiconductor modification. The combination of oxide and TiO_2 can broaden the light absorption threshold of TiO_2 [62], effectively improve the separation effect of charge in TiO_2 semiconductors and improve the photocatalytic activity [63,64] and photocatalytic efficiency [65].

Scholars continue to explore TiO_2 modifications in order that it can effectively use visible light to reduce the recombination rate of electron holes and to effectively improve the transmission efficiency of photons and enhance TiO_2 photocatalysis with the objective of improving the organic matter mineralization efficiency of the system.

4. Ozone Micro/Nanobubble Technology

In advanced oxidation processes, ozone has strong oxidability and fast reaction speed and causes no secondary pollution to the environment. Therefore, ozone is widely used in drinking water treatment [66,67], printing and dyeing wastewater treatment [6,13,68] and coal chemical wastewater [69–71]. Ozone can decompose in water to produce stronger oxidizing substances than itself, such as hydroxyl radicals, which can effectively oxidize and degrade organic pollutants in water [9]. Although ozone has high oxidability, its solubility in water is not high and its stability is poor, which will reduce the elimination and mineralization of refractory organics by ozone [7]. Therefore, improving the solubility and mass transfer efficiency of ozone in water is an important problem to be solved.

4.1. Characteristics of Micro/Nanobubbles

Micro/nano bubble refers to the bubble between micron bubble (diameter of 10–50 μm) and nano bubble (diameter of less than 200 nm); different scholars have different definitions of the limit range of its diameter. Generally, bubbles with a diameter of less than 50 μm are considered as micro-nano bubbles, in which microbubbles and nanobubbles are small bubbles with diameters of 10–50 μm and <200 nm, respectively, while bubbles with diameters of more than 50 μm are considered as conventional large bubbles [72–76]. These advantages are mainly reflected in the following aspects:

(1) Large specific surface area. According to the formula S/V = 3/r, the specific surface area per unit volume of a bubble is inversely proportional to the bubble radius. The diameter of a micro/nanobubble is small, and the specific surface area is large. For example, the specific surface area of a bubble with a radius of 1 μm has 1000 times the normal bubble of 1 mm [77]. The larger the specific surface area is, the larger the contact area with the liquid, which corresponds to a higher reaction rate.

(2) Long hysteresis in water. Micro/nanobubbles have smaller diameters than ordinary bubbles. This unique advantage makes them float slowly in the process of gas-liquid mass transfer and have a longer residence time in the liquid [78].

(3) The zeta potential at the gas-liquid interface is high. The surface of a bubble in pure water is rich in negative charges [79]. The zeta potential measured in water of micro/nanobubbles with oxygen as the gas source ranged from −45 to −34 mV, compared to −20 to −17 mV in water of ordinary large bubbles.

(4) Self-rupture produces a mass of free radicals. Micro/bubbles can shrink and burst without external stimulation, and instantly release a large amount of ·OH [80], which has high oxidation potential and can selectively oxidize organic pollutants in water, such as phenol. Because of this characteristic, micro/nanobubbles can be used for the treatment of refractory water.

4.2. Ozone Micro/Nanobubble Technology

In view of the above characteristics of micro/nanobubbles, a formation diagram of ·OH at the gas-liquid interface of a microbubble [81] is shown in Figure 2. The collapse and autolysis of MNBs and the large accumulation of ions at the gas-liquid interface of bubbles are the key factors for the generation of ·OH. At the same time, the higher compatibility of the bubble surface creates good conditions for the improvement of ozone solubility in O_3 MNBs; hence, O_3 MNBs generate more hydroxyl radicals when they break [82].

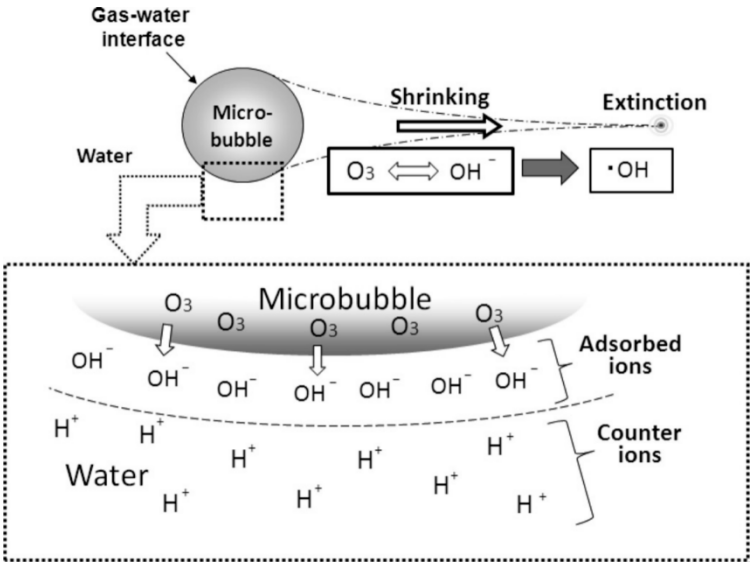

Figure 2. Mechanism of hydroxyl radical production by ozone microbubbles [81]. Reprinted with permission from Ref. [81].

Hydroxyl radicals have a strong oxidation ability and can quickly react with electronic sites that are rich in organic matter in water, trigger complex free radical chain reactions and degrade most organic matter into H_2O, CO_2 and inorganic salts. During the degradation of phenol, ·OH reacts with the electron hole on the phenol molecule to produce the intermediate product hydroquinone and finally mineralize the phenol [83].

4.3. Application of Ozone Micro/Nanobubbles to the Degradation of Phenolic Pollutants

The ozone oxidation process has been widely studied by researchers in the field of water treatment [84–86], but it is limited by ozone mass transfer and oxidation selectivity in practical applications. Therefore, many researchers have focused on using microbubble processes to enhance the mass transfer efficiency and utilization of ozone [87–89].

(1) Microbubbles can effectively improve the mass transfer efficiency of ozone and the yield of ·OH, and then improve the mineralization efficiency of organic matter [18,90,91]. The adjustment of the hydrodynamic behavior of ozone microbubbles can increase the degradation rate of organic matter to realize an obvious removal effect. Micro/nanobubbles can enhance ozone mass transfer and accelerate ozone decomposition to produce ·OH [90]. As the ozone generation rate increases, the partial pressure of ozone also increases, thereby improving the mass transfer of ozone [92].

(2) The oxidation mechanism of ozone microbubbles on organic matter is an indirect oxidation process dominated by the oxidation of free radicals [90,93,94]. Ozone can be oxidized effectively with most organic matter, and micro/nanobubbles can improve oxidation efficiency of ozone to organic matter [90], this is because ozone microbubbles can produce non-selective ·OH, enabling organic matter to achieve more active oxidation degradation [82]. The oxidation of organic matter by ozone microbubbles is an indirect oxidation process dominated by free radical (·OH), which is different from the direct oxidation of organic matter by conventional bubbles [21].

(3) The collapse of micro/nanobubbles can play an important role in the decomposition of organic matter [95–97]. Collapsing air micro/nanobubbles can lead to decomposition of phenol, and upon collapse, a large amount of ·OH is released, which plays an important role in the degradation of phenol [98,99]. At the same time, the pH of the solution and the type of gas in the micro/nanobubbles also play an important role in the degradation of phenol. The pH value directly affects the number of free radicals that are generated when an oxygen micro/nanobubble breaks and the degree of ionization of phenol in the aqueous solution [95,98].

(4) Hydroxyl radicals have a higher standard redox potential than ozone and hydrogen peroxide [3,100,101]. The addition of H_2O_2 enhances the formation of ·OH in the system, which may be because the added H_2O_2 oxidant can react with ·OH to form ·OH and promote the formation of ·OH [102]. In addition, it can effectively inhibit the compound reaction of free radicals and enable ·OH to decompose organic matter efficiently [17].

In conclusion, the degradation of phenolic pollutants by the ozone micro/nanobubble method is better than that by traditional bubble methods, which can be combined with other processes to improve the degradation rate of organic compounds.

Micro/nanobubbles have the same characteristics as traditional bubbles. Ozone micro/nanobubble technology can solve the problems of low ozone utilization, selectivity of ozone oxidation and slow gas-liquid mass transfer rate in traditional ozone catalytic oxidation technology for water treatment [82,103]. The presence of microbubbles can accelerate the decomposition of hydroxyl radicals of ozone [17,18] and greatly improve the mineralization efficiency of refractory organics [19–21]. Moreover, micro/nanobubbles can also keep the catalyst in a dynamic discrete state, which effectively increases the contact frequency between the catalyst and refractory organics [12,22,23], contributes to the oxidative degradation of refractory organics and gives ozone catalytic oxidation technology broader application prospects in the field of water treatment.

5. Catalyst and Micro/Nanobubble Mechanism

5.1. Synergistic Interaction between Nanoparticles and Micro/Nanobubbles

When using microbubble processes in combination with photocatalytic oxidation, the catalytic oxidation performance can be promoted without modification or doping of the catalyst, which benefits from the synergy between nanoparticles and microbubbles.

Nanobubbles can facilitate nanoparticle substrate adsorption, which occurs by capillary bridge-assisted MNB nanoparticle adhesion, and helps form a contact liner to stabilize bubbles on the three-phase interface [104]. At the same time, MNBs have a high specific surface area, which makes them adsorb with organic matter and interact with nanoparticles on the surface [105].

Fan et al. [106] evaluated MNB-UV/TiO_2 in the process of advanced treatment of urban secondary wastewater. The purification process in the mixed system consists of two stages (as shown in Figure 3), and these two stages exist synchronously forming a macro perspective. First, MNBs not only have the ability to capture organic pollutants and carriers [107] but also can increase the amount of oxygen in photocatalytic reactions. In the first stage, in the spaces between MNBs and TiO_2 a photocatalytic region arises that can enhance the degradation of organic matter. The rise, contraction and collapse of bubbles cause MNBs-TiO_2 to form in the second stage of the interaction; the pressure in each bubble increases with the decrease in the bubble's radius [108]; the MNBs exchange heat very fast with the surroundings; and each bubble has a negative charge over a wide pH range [109]. At this time, the extremely high concentration ion field provides favorable conditions for the generation of strongly oxidizing radicals such as ·OH.

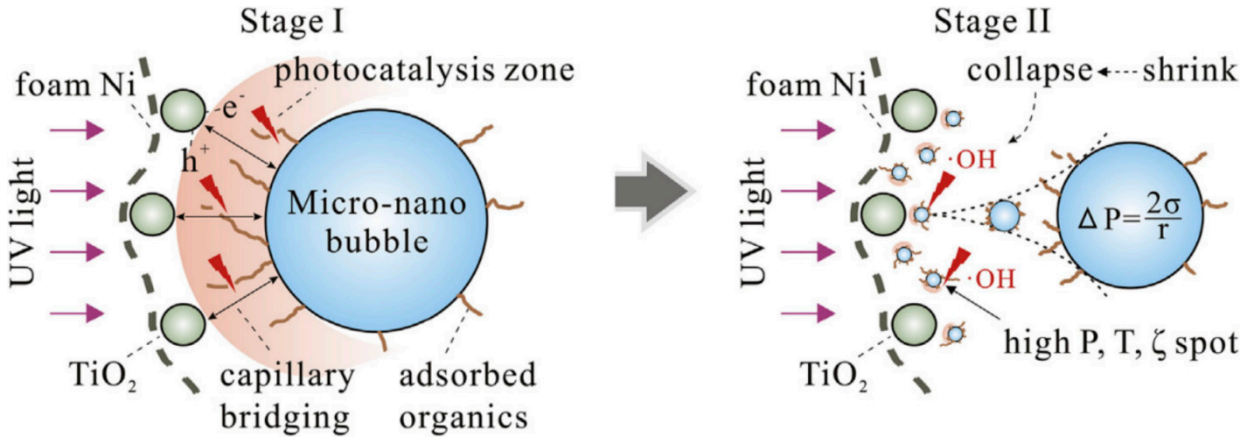

Figure 3. Two stages of purification in the MNB-UV/TiO_2 hybrid system. P is the pressure, T is the temperature, ζ is the electric potential, ΔP is the Laplace pressure, σ is the surface tension and r is the bubble radius [106] ("foam Ni" is a base material for TiO_2 attachment). Reprinted with permission from Ref. [106].

5.2. Nanoparticles Promote the Formation and Stabilization of Micro/Nanobubbles

The interaction between the bulk nanobubble solution and nanoparticles occurs through new nucleation on nanoparticles rather than collision [110]. The high-energy barrier and colloidal stability between nanoparticles [111] can effectively prevent their aggregation in dilute solution. At the same time, the addition of nanoparticles can significantly enhance the formation and stability of microbubbles [112] because the gas molecules in the solution are adsorbed on the surface of nanoparticles, and their nucleation is easier than homogeneous nucleation [113].

According to classical nucleation theory [114], the free energy that is required to form a bubble is:

$$\Delta G = -V\Delta p + A\gamma$$

where Δp is the pressure difference across the interface, γ is the surface tension of the gas–liquid interface, V is the bubble volume and A is the area of the gas-liquid interface. However, for homogeneous nucleation, the free energy that is required to form a spherical bubble with radius R is: $\Delta G = -V\Delta p + 4\pi R^2\gamma$. When the bubble reaches equilibrium, the critical radius obeys the Young–Laplace equation: $R^* = 2\gamma/\Delta p$. This depends on the bubble size, which is also supported by the findings of Zhang [110] and others that the

mixing of nanoparticles and nanobubbles increases the concentration of NBs in the solution and the interaction between plate nanobubbles and nanoparticles.

As shown in Figure 4, an independent measurement method was established to examine the influence of nanocrystals on NB formation when pure nitrogen was used to produce NBs. Xiao et al. [115] found that, regardless of the pressure, the addition of TiO_2 nanoparticles can significantly increase the concentration of micro/nanobubbles, and the effect of TiO_2 nanoparticles on the concentration of micro/nanobubbles is more significant, namely, that the concentration can be increased by 5 times in the pressurized system. A study by Zhang [110] confirmed that the addition of nanosolids can either increase bubble nucleation or provide additional nucleation centers to increase the NB concentration and that pressurization can increase the concentration of dissolved gas in the solution, which can be followed by appropriate decompression to promote homogeneous nucleation of bubbles and, thus, enhance the concentration of bubbles in the solution. The addition of nanosolids can promote the heterogeneous nucleation of bubbles and greatly increase the NB concentration.

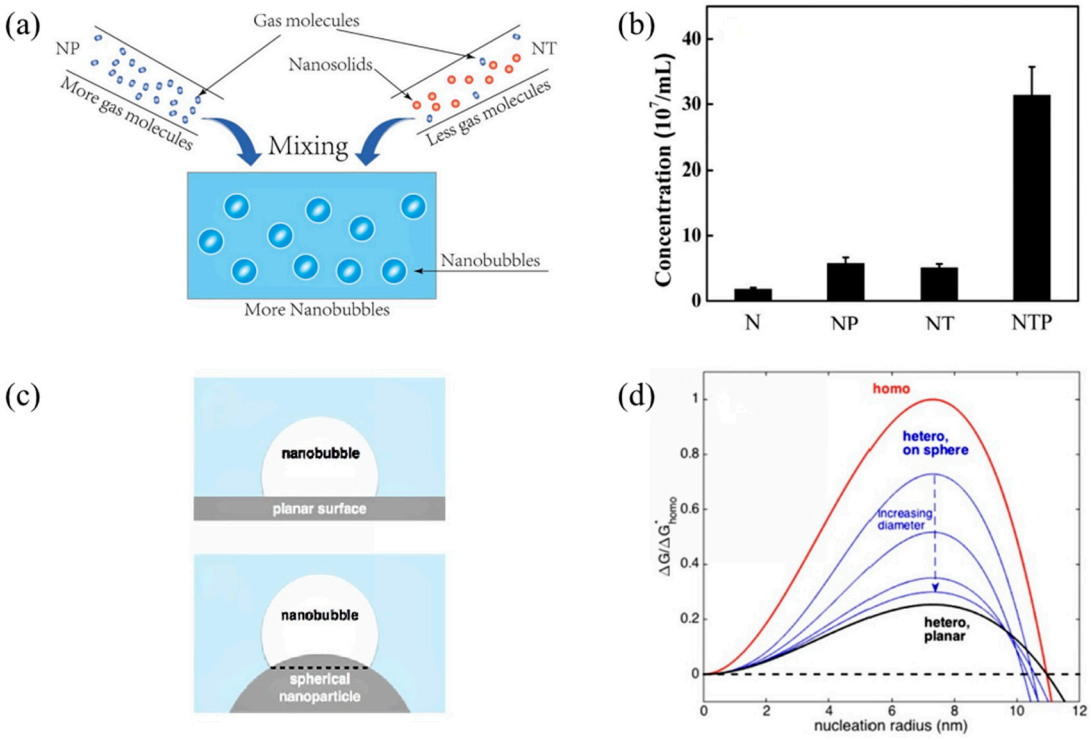

Figure 4. (**a**) A nanoparticles and nanobubbles mixed solution, (**b**) the effect of nanoparticles on nanobubbles, (**c**) the nucleation of nanobubbles at planar and solid/gas interfaces and (**d**) the energy barrier that prevents nucleation for homogeneous nucleation, which shows that nucleation on smaller nanoparticles requires more energy [110,115]. (N—Na_2CO_3; NP—pressurized N; NT—$Na_2CO_3$$^+$ titanium dioxide; NTP—pressurized NT), reprinted with permission from Refs. [110,115].

6. Degradation Mechanism of Organic Matter in the Catalyst-O_3 Micro/Nanobubble System

6.1. Generation of ·OH

The presence of microbubbles is an important factor for the conversion of ozone to ·OH. The formation of ·OH in the formed ozone microbubbles is largely due to the increase in the absolute value of the electromotive force at the liquid interface when the microbubbles gradually shrink [116], and large amounts of OH^- and H^+ rapidly accumulate at the bubble interface. Ozone interacts with hydroxyl ions that are adsorbed at the gas-water interface to generate ·OH. The reaction formula is as shown in Figure 5.

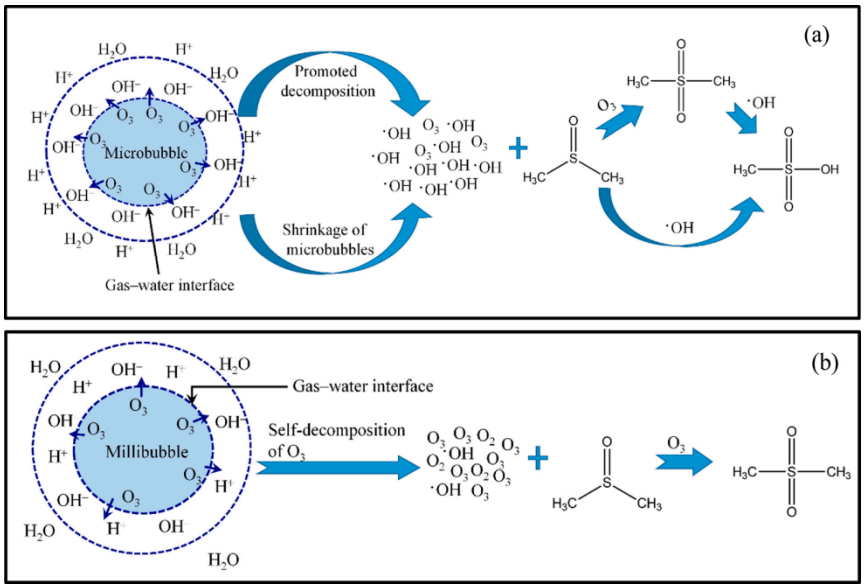

Figure 5. Proposed mechanisms of DMSO degradation by (**a**) OMBs and (**b**) OMLBs [12]. (DMSO—dimethyl sulfoxide; OMBs—ozone microbubbles; OMLBs—ozone millibubbles). Reprinted with permission from Ref. [12].

Jabesa et al. [12], based on a comparative test of ozone oxidation under traditional bubbles and oxidative degradation of dimethyl sulfoxide by ozone micro/nanobubbles, proved that the enrichment of OH^- on the surface of microbubbles leads to a negative charge on the surface of the microbubble (as shown in Figure 5a), which promotes the self-decomposition of ozone into chiral ·OH. At the same time, the shrinkage and collapse of microbubbles is another important way to produce ·OH. Ozone is transmitted, and the self-decomposition pathway in a bubble system is different from that in a microbubble system (as shown in Figure 5b). Ozone is rapidly decomposed into oxygen due to its instability, forming less ·OH under highly alkaline conditions and less in the traditional bubble system.

6.2. Mass Transfer and Decomposition of O_3

According to Henry's law, the solubility of ozone is proportional to the partial pressure and total pressure in the system [117]. Although ozone has strong oxidization properties, its available solubility is very small in practical use. Therefore, improving the solubility and mass transfer efficiency of ozone in water is an important problem to be solved. When microbubbles rise in a reactor, they break due to the reduction of their volume and the increase of their specific surface area and surface charge density. The relationship between diameter and pressure can be described by the Young–Laplace equation:

$$P = P_1 + \frac{4\delta}{d}$$

where P is the gas pressure, P_1 is the liquid pressure, δ is the liquid apparent tension and d is the bubble diameter.

A larger interfacial area and higher internal pressure endow microbubbles with the potential to improve ozone gas–liquid mass transfer. As shown in Figure 6a, according to the dual-mode theoretical diagram of ozone mass transfer, the gas–liquid interface is located between the gas film and the liquid film, and there is mass transfer resistance at the gas–liquid interface. The relationship between the theoretical mass transfer coefficient and bubble diameter is shown in Figure 6b. When micro/nanobubbles are used for mass transfer, the bubble particle size is in the order of microns and is less than 100 μm. It is generally believed that there is no mass transfer resistance in micro/nanobubbles.

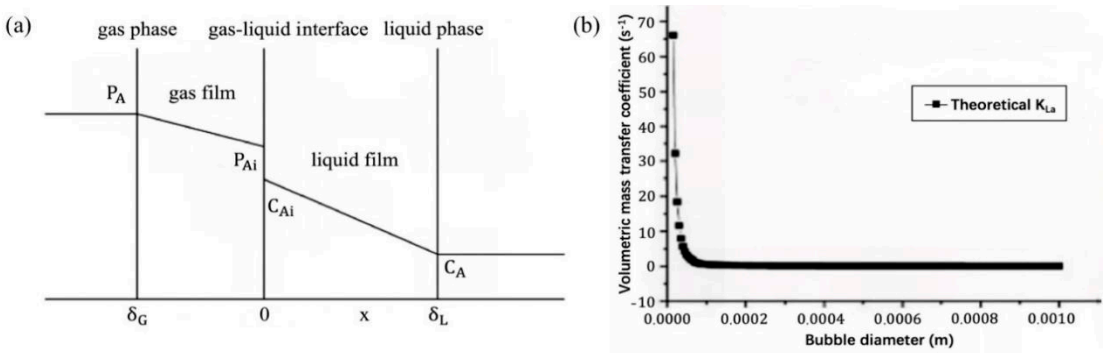

Figure 6. (**a**) A two−mode theoretical diagram of ozone mass transfer [82] and (**b**) the theoretical volumetric mass transfer coefficient values for various bubble diameters [118]. Reprinted with permission from Refs. [82,118].

Yao et al. [118] measured and compared the volumetric mass transfer coefficient values of microbubbles and traditional bubbles and demonstrated that microbubbles enhance mass transfer. Under the same gas flow rate, the volume mass transfer coefficient of microbubbles is 32.59% higher than that of conventional bubbles. Figure 7 shows the changes in the dissolved oxygen concentration with time in the microbubble system and in the traditional bubble system. The final stable value of the microbubbles is significantly higher than that of the traditional bubbles.

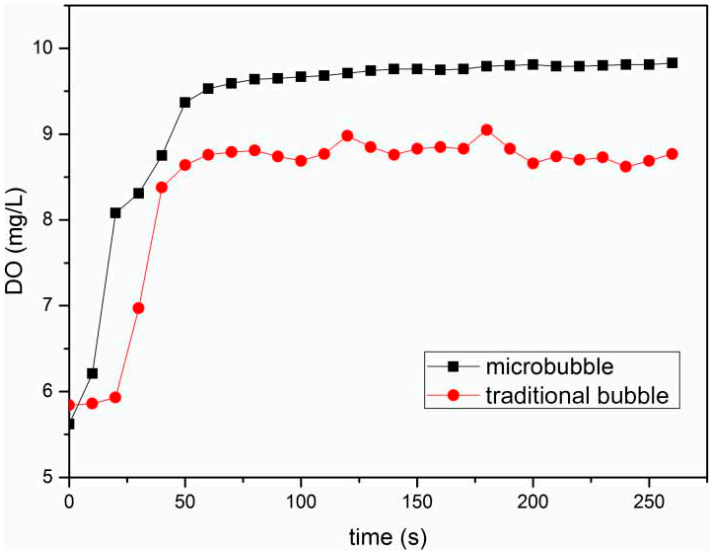

Figure 7. Variation in DO concentration at a gas flow rate of 0.67 L/min [118]. (DO—dissolved oxygen). Reprinted with permission from Ref. [118].

6.3. Synergistic Mechanism

When the catalyst ozone microbubble system oxidizes and degrades organics, there is a synergy between the adsorption of organics by the catalyst and the oxidation of organics by ozone microbubbles, but the degradation of organics in the catalyst ozone microbubble system is not a simple superposition of microbubble ozonation and catalyst adsorption.

Zhang et al. [119] proposed four possible synergistic mechanism processes through MB-O_3-Cu and Mn/Na_2SiO_3 system experiments (Figure 8): (1) microbubbles adhere to the surface of the catalyst and inside the pores; (2) microbubbles collapse, burst and release large amounts of O_3 and ·OH; (3) O_3 reacts at the surface active center of the catalyst to produce ·OH; and (4) oxidative degradation of acid scarlet 3R macromolecular and small organic acids by O_3 and ·OH occurs. Figure 8 illustrates the catalytic process mechanism of the MB-catalyst-O_3 system. Oxygen vacancies on the catalyst surface are occupied

by adsorbed water molecules to generate $–OH_2^+$ (process 1). Microbubbles adhere to the surface of the catalyst and the insides of the pores, and the collapse and rupture of microbubbles release a large amount of O_3 and ·OH (process 2). O_3 and $–OH_2^+$ on the catalyst surface form the six-membered rings under the action of an electrostatic force and hydrogen bonding (process 3). Each six-membered ring decomposes into ·OH due to its instability, and HO_3· is further decomposed into OH and O_2 (process 4). O_3 and ·OH contact to form a five membered ring (process 5) and then convert to O_2 and $–HO_2–$ (process 6). O_3 and $–HO_2–$ react to generate $–O_2^-$· and HO_3· (process 7). O_2 is released by $–O_2^-$ and the surfactant site is regenerated (process 8).

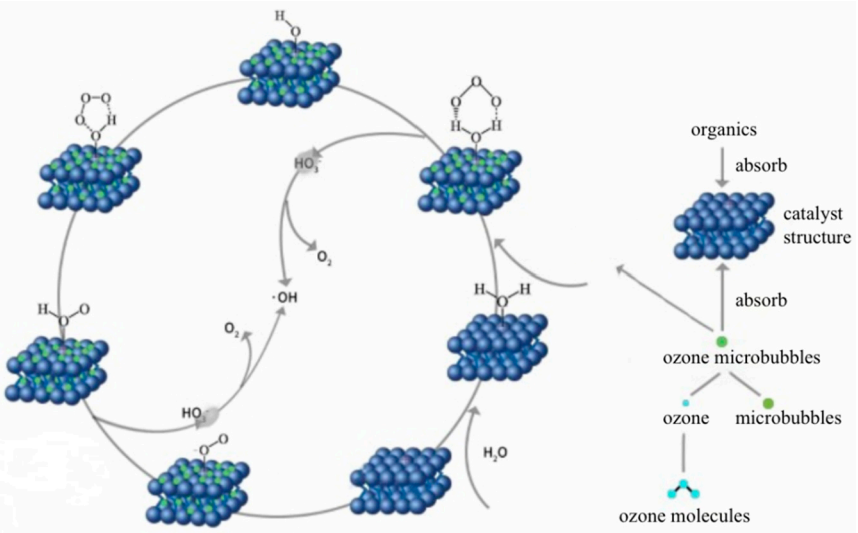

Figure 8. Mechanism of the catalytic process in the MB-catalyst-O_3 system [120]. Reprinted with permission from Ref. [120].

6.4. Additive Effect of H_2O_2

The addition of H_2O_2, which is a strong oxidant, can significantly improve the decomposition rate of organic matter. This is because H_2O_2 photolysis can produce ·OH, which enhances the decomposition of organic matter:

$$H_2O_2 + h\nu \rightarrow 2{\cdot}OH$$

H_2O_2 can be transformed and quenched with ·OH by the following reaction [121]:

$$2{\cdot}OH \rightarrow H_2O_2$$

$$\cdot OH + H_2O_2 \rightarrow HO_2{\cdot} + H_2O$$

In the presence of H_2O_2, the ozone oxidation system can generate HO in water and produce HO_2^- and H_3O^+, where HO_2^- reacts again to form ·OH [102] with strong oxidation:

$$O_3 + H_2O_2 \rightarrow \cdot OH + HO_2{\cdot} + O_2$$

$$H_2O_2 + H_2O \rightarrow HO_2^- + H_3O^+$$

$$O_3 + HO_2^- \rightarrow O_2 + O_2^- + \cdot OH$$

In addition, the surface of rutile TiO_2 adsorbs H_2O_2 which can be used as a catalyst to promote the formation of ·OH. There is a good correlation between the amount of ·OH that is added to the solution and the apparent oxidation ability; upon exposure to light, TiO_2

forms surface holes, and ·OH is captured on the TiO_2 surface. Under neutral pH conditions, ·OH dissociates and adsorbs in the form of trapped holes [10]:

$$\cdot OH \leftrightarrow \cdot O^- + H^+$$

$$\cdot OH + Ti^{4+} \leftrightarrow Ti^{4+}O\cdot^- + H^+$$

In the rutile TiO_2/H_2O_2 system, the addition of H_2O_2 greatly increases the content of ·OH, which may be due to TiO_2-surface-adsorbed H_2O_2, which can promote the generation of ·OH [11,122]. The formation of ·OH by the additive effect of TiO_2 and H_2O_2 plays a synergistic role in the degradation of organic compounds dominated by ·OH.

In conclusion, the exploration and verification results that are discussed above provide references for the application of catalyst ozone micro/nanobubble systems in the treatment of refractory organics.

7. Prospects for Nanoparticles/Ozone Micro/Nanobubbles Systems

Micro/nanobubbles have been widely used in many fields due to their unique properties. Although many excellent results have been obtained and substantial progress has been made in the investigation of catalyst and ozone micro/nanobubbles, this research is still in its infancy, and many challenges remain.

First, the production of controllable MNBs with smaller sizes and higher concentrations is crucial to the application of catalysts and ozone micro/nanobubbles.

Second, the interaction of the catalyst and ozone micro/nanobubbles is limited by the nucleation and collision of micro/nanobubbles. It is necessary to develop new techniques with both higher spatial resolutions and kinetic models.

Third, although several models of the utilization of micro/nanobubbles have been proposed, their long lifetimes remain to be satisfactorily explained. Especially in sludge reduction and river governance, the presence of microbubbles creates an aerobic environment for the sediment, provides conditions for the growth of aerobic bacteria and strengthens the decomposition of organic matter in the sediment to solve the river eutrophication problem.

Finally, it is believed that catalyst/ozone micro/nanobubbles systems have strong prospects in a wide range of applications, especially the degradation of refractory organic matter.

Author Contributions: Conceptualization, W.X. and H.Z.; validation, T.L., W.Y. and S.D.; formal analysis, W.X.; investigation, X.W.; resources, B.W.; writing—original draft preparation, H.Z.; writing—review and editing, W.X.; visualization, B.W.; supervision, T.L.; project administration, W.Y.; funding acquisition, W.X. All authors have read and agreed to the published version of the manuscript.

Funding: This research was funded by the National Natural Science Foundation of China (52004197) and the Natural Science Basic Research Program of Shaanxi (2020JQ-667).

Institutional Review Board Statement: Not applicable.

Informed Consent Statement: Not applicable.

Data Availability Statement: Not applicable.

Acknowledgments: The authors acknowledge the Zhangjiang Lab, Shanghai Advanced Research Institute, Chinese Academy of Sciences. Thanks to Zhang Lijuan and Hu Jun for revising the paper.

Conflicts of Interest: The authors declare no conflict of interest.

References

1. Takeuchi, N.; Ishibashi, N.; Sugiyama, T.; Kim, H.H. Effective utilization of ozone in plasma-based advanced oxidation process. *Plasma Sources Sci. Technol.* **2018**, *27*, 055013. [CrossRef]
2. Ozturk, H.; Barisci, S.; Turkay, O. Paracetamol degradation and kinetics by advanced oxidation processes (AOPs): Electro-peroxone, ozonation, goethite catalyzed electro-fenton and electro-oxidation. *Environ. Eng. Res.* **2021**, *26*, 180332. [CrossRef]
3. Takeuchi, N.; Mizoguchi, H. Study of optimal parameters of the H_2O_2/O_3 method for the decomposition of acetic acid. *Chem. Eng. J.* **2017**, *313*, 309–316. [CrossRef]

4. Malik, S.N.; Ghosh, P.C.; Vaidya, A.N.; Mudliar, S.N. Hybrid ozonation process for industrial wastewater treatment: Principles and applications: A review. *J. Water Process Eng.* **2020**, *35*, 101193. [CrossRef]
5. Yan, S.; Sun, J.; Sha, H.; Li, Q.; Nie, J.; Zou, J.; Chu, C.; Song, W. Microheterogeneous Distribution of Hydroxyl Radicals in Illuminated Dissolved Organic Matter Solutions. *Environ. Sci. Technol.* **2021**, *55*, 10524–10533. [CrossRef] [PubMed]
6. Liu, Y.; Guo, P. Pilot-scale Study on Treatment of Printing and Dyeing Wastewater by Two-Stage Catalytic Ozonation. *Technol. Water Treat.* **2017**, *43*, 73–75.
7. Khataee, A.; Rad, T.S.; Fathinia, M.; Joo, S.W. Production of clinoptilolite nanorods by glow discharge plasma technique for heterogeneous catalytic ozonation of nalidixic acid. *Rsc. Adv.* **2016**, *6*, 20858–20866. [CrossRef]
8. Ghuge, S.P.; Saroha, A.K. Catalytic ozonation for the treatment of synthetic and industrial effluents—Application of mesoporous materials: A review. *J. Environ. Manag.* **2018**, *211*, 83–102. [CrossRef] [PubMed]
9. Fu, L.Y.; Wu, C.Y.; Zhou, Y.X.; Zuo, J.; Song, G.Q.; Tan, Y. Ozonation reactivity characteristics of dissolved organic matter in secondary petrochemical wastewater by single ozone, ozone/H_2O_2, and ozone/catalyst. *Chemosphere* **2019**, *233*, 34–43. [CrossRef]
10. Zhang, J.; Nosaka, Y. Quantitative Detection of OH Radicals for Investigating the Reaction Mechanism of Various Visible-Light TiO_2 Photocatalysts in Aqueous Suspension. *J. Phys. Chem. C* **2013**, *117*, 1383–1391. [CrossRef]
11. Tang, J.; Chen, Y.; Dong, Z. Effect of crystalline structure on terbuthylazine degradation by H_2O_2-assisted TiO_2 photocatalysis under visible irradiation. *J. Environ. Sci.* **2019**, *79*, 153–160. [CrossRef]
12. Jabesa, A.; Ghosh, P. A comparative study on the removal of dimethyl sulfoxide from water using microbubbles and millibubbles of ozone. *J. Water Process Eng.* **2021**, *40*, 101937. [CrossRef]
13. Yu, S.; Tang, Z.; Zhang, Y.; Hong, F. Case Analysis of Printing and Dyeing Wastewater Treatment Project with a Commbined Process of MBR and Ozonation. *China Water Wastewater* **2019**, *35*, 104–107.
14. Liu, Y.; Liu, Y.J.; Duan, J.Q.; Zhou, L. The removal characteristics analysis of volatile phenols in semi-coking wastewater after physicochemical-biochemical combination treatment. *Environ. Pollut. Control.* **2016**, *38*, 34–38.
15. Maurya, I.C.; Singh, S.; Srivastava, P.; Bahadur, L. Green synthesis of TiO_2 nanoparticles using *Bixa orellana* seed extract and its application for solar cells. *Sol. Energy* **2019**, *194*, 952–958. [CrossRef]
16. Maurya, I.C.; Senapati, S.; Singh, S.; Srivastava, P.; Maiti, P.; Bahadur, L. Effect of Particle Size on the Performance of TiO_2 Based Dye-Sensitized Solar Cells. *Chemistryselect* **2018**, *3*, 9872–9880. [CrossRef]
17. Matsuura, R.; Kometani, N.; Horibe, H.; Shirafuji, T. Enhanced decomposition of toxic pollutants by underwater pulsed discharge in the presence of hydrogen peroxide and microbubbles. *Jpn J. Appl. Phys.* **2022**, *61*, SA1003. [CrossRef]
18. Zeng, S.; Yang, Y.; Zhang, N.; Ye, J.; Huang, Y.; Xiao, M. Enhanced ozone degradation of the p-nitrophenol wastewater by rotating-microbubble reactor. *Chem. Ind. Eng. Prog.* **2021**, *40*, 4091–4099.
19. Xia, Z.; Hu, L. Treatment of Organics Contaminated Wastewater by Ozone Micro-Nano-Bubbles. *Water* **2019**, *11*, 55. [CrossRef]
20. Shin, W.-T.; Chang, S.N. Organic Pollutants Degradation Using Pulseless Corona Discharge: Application in Ultrapure Water Production. *Environ. Eng. Res.* **2005**, *10*, 144–154. [CrossRef]
21. Du, M.; Wang, Y.; Sun, X. Mechanism and efficiency of ozone microbubble treatment of organic wastewater. *Chem. Ind. Eng. Prog.* **2021**, *40*, 6907–6915.
22. Zhang, W.P.; Li, G.Y.; Liu, H.L.; Chen, J.Y.; Ma, S.T.; An, T.C. Micro/nano-bubble assisted synthesis of Au/TiO_2@CNTs composite photocatalyst for photocatalytic degradation of gaseous styrene and its enhanced catalytic mechanism. *Environ. Sci.-Nano* **2019**, *6*, 948–958. [CrossRef]
23. Zhang, J.; Huang, G.Q.; Liu, C.; Zhang, R.N.; Chen, X.X.; Zhang, L. Synergistic effect of microbubbles and activated carbon on the ozonation treatment of synthetic dyeing wastewater. *Sep. Purif. Technol.* **2018**, *201*, 10–18. [CrossRef]
24. Wang, Y.; Zhao, Z.; Wang, Y.; Hua, J.; Zhang, D.; Zhang, H.; Jiao, S. Study on the Pollution Characteristics of Typical Textile Dyeing Sludge (TDS) in China. *J. Ecol. Rural Environ.* **2020**, *36*, 1598–1604.
25. He, J.; Fu, H.Y.; Jiang, W. Performance promotion of Ag_2O photocatalyst by particle size and crystal surface regulation. *New J. Chem.* **2020**, *44*, 10719–10728. [CrossRef]
26. Wu, X.; Han, H.; Fang, F. Analysis on Innovative Technology for High Phenol and Ammonia Treatment of Wastewater from Coal Chemical Industry. *China Water Wastewater* **2017**, *33*, 26–32.
27. Liu, J.; Wu, T.; Li, J.; Zeng, G.; Yang, C.; Huang, H.; Yin, D. Research progress on the deep purification of phenol-containing wastewater by advanced carbon materials. *Ind. Water Treat.* **2020**, *40*, 1017–1023.
28. Zhang, J.X.; Xie, M.L.; Zhao, H.Y.; Zhang, L.R.; Wei, G.F.; Zhao, G.H. Preferential and efficient degradation of phenolic pollutants with cooperative hydrogen-bond interactions in photocatalytic process. *Chemosphere* **2021**, *269*, 129404. [CrossRef] [PubMed]
29. Xiang, W.R.; Qu, R.J.; Wang, X.H.; Wang, Z.Y.; BinJumah, M.; Allam, A.A.; Zhu, F.; Huo, Z.L. Removal of 4-chlorophenol, bisphenol A and nonylphenol mixtures by aqueous chlorination and formation of coupling products. *Chem. Eng. J.* **2020**, *402*, 126140. [CrossRef]
30. Sas, O.G.; Castro, M.; Dominguez, A.; Gonzalez, B. Removing phenolic pollutants using Deep Eutectic Solvents. *Sep. Purif. Technol.* **2019**, *227*, 115703. [CrossRef]
31. Liu, R.; Wang, W.; Shi, C.; Ma, C.P. Microwave—Induced catalytic oxidation of two—Component (phenol, p-nitrophenol) phenolic wastewater. *Abstr. Pap. Am. Chem. Soc.* **2018**, *255*, 125066.

32. Guo, T.T.; Yang, S.; Chen, Y.N.; Yang, L.; Sun, Y.N.; Shang, Q.K. Photocatalytic kinetics and cyclic stability of photocatalysts Fe-complex/TiO_2 in the synergistic degradation of phenolic pollutants and reduction of Cr(VI). *Environ. Sci. Pollut. Res.* **2021**, *28*, 12474. [CrossRef] [PubMed]
33. Ministry of Ecology and Enviroment of the People's Republic of China. China Ecological and Environmental Statistical Annual Report 2019. Available online: https://www.mee.gov.cn/hjzl/sthjzk/sthjtjnb/202108/t20210827_861012.shtml (accessed on 1 April 2022).
34. Feng, C.; Chen, Z.Y.; Jing, J.P.; Hou, J. The photocatalytic phenol degradation mechanism of Ag-modified ZnO nanorods. *J. Mater. Chem. C* **2020**, *8*, 3000–3009. [CrossRef]
35. Pratarn, W.; Pornsiria, T.; Thanitb, S.; Tawatchaic, C.; Wiwutc, T. Adsorption and ozonation kinetic model for phenolic wastewater treatment. *Chin. J. Chem. Eng.* **2011**, *19*, 76–82. [CrossRef]
36. Siracusa, L.; Gresta, F.; Sperlinga, E.; Ruberto, G. Effect of sowing time and soil water content on grain yield and phenolic profile of four buckwheat (Fagopyrum esculentum Moench.) varieties in a Mediterranean environment. *J. Food Compos. Anal.* **2017**, *62*, 1–7. [CrossRef]
37. *GB18918-2002*; Pollutant Discharge Standards for Urban Sewage Treatment Plants. State Environmental Protection Administration: Beijing, China, 2002.
38. Kim, S.; Sung, B.H.; Kim, S.C.; Lee, H.S. Genetic incorporation of L-dihydroxyphenylalanine (DOPA) biosynthesized by a tyrosine phenol-lyase. *Chem. Commun.* **2018**, *54*, 3002–3005. [CrossRef] [PubMed]
39. Wilson, R.M.; Tfaily, M.M. Advanced Molecular Techniques Provide New Rigorous Tools for Characterizing Organic Matter Quality in Complex Systems. *J. Geophys. Res.-Biogeosci.* **2018**, *123*, 1790–1795. [CrossRef]
40. Contreras-Bustos, R.; Cardenas-Mijangos, J.; Dector-Espinoza, A.; Rodriguez-García, A.; Montoya-Herrera, L.; Jiménez-Becerril, J. Treatment of wastewater from the petrochemical industry by chemical Fenton process. *Rev. Mex. Ing. Quim.* **2020**, *19*, 523–532. [CrossRef]
41. Guo, Y.; Guo, Y.; Wang, X.; Liang, P.; Li, P.; Li, X. Research on the combined process and its application of environmental control technology and photocatalytic. *Ind. Water Treat.* **2017**, *37*, 5–10.
42. Al-Madanat, O.; AlSalka, Y.; Ramadan, W.; Bahnemann, D.W. TiO_2 Photocatalysis for the Transformation of Aromatic Water Pollutants into Fuels. *Catalysts* **2021**, *11*, 317. [CrossRef]
43. Shirini, F.; Abedini, M.; Seddighi, M. TiO_2 and Its Derivatives as Efficient Catalysts for Organic Reactions. *J. Nanosci. Nanotechnol.* **2016**, *16*, 8208–8227. [CrossRef]
44. Zhao, X.; Ismoilov, B.; Li, Y.; Li, X.; Zhang, H.; Hu, T. Research Status and New Progress of Advanced Oxidation Technology for Wastewater Treatment. *Technol. Water Treat.* **2018**, *44*, 7–10, 16.
45. Molla, M.A.I.; Furukawa, M.; Tateishi, I.; Katsumata, H.; Kaneco, S. Solar photocatalytic decomposition of Probenazole in water with TiO_2 in the presence of H_2O_2. *Energy Sources Part A-Recovery Util. Environ. Eff.* **2018**, *40*, 2432–2441. [CrossRef]
46. Song, T.H.; Li, R.; Li, N.; Gao, Y.J. Research Progress on the Application of Nanometer TiO_2 Photoelectrocatalysis Technology in Wastewater Treatment. *Sci. Adv. Mater.* **2019**, *11*, 158–165. [CrossRef]
47. Tang, Y.C.; Hu, C.; Wang, Y.Z. Recent advances in mechanism and kinetice of TiO_2 photocatalysis. *Prog. Chem.* **2002**, *14*, 192–199.
48. Qiao, L.; Xie, F.; Xie, M.; Gong, C.; Wang, W.; Gao, J. Characterization and photoelectrochemical performance of Zn-doped TiO_2 films by sol-gel method. *Trans. Nonferrous Met. Soc. China* **2016**, *26*, 2109–2116. [CrossRef]
49. Niu, T.; Chen, W.; Cheng, H.; Wang, L. Grain growth and thermal stability of nanocrystalline Ni-TiO_2 composites. *Trans. Nonferrous Met. Soc. China* **2017**, *27*, 2300–2309. [CrossRef]
50. Hashemzadeh, M.; Raeissi, K.; Ashrafizadeh, F.; Hakimizad, A.; Santamaria, M. Incorporation mechanism of colloidal TiO_2 nanoparticles and their effect on properties of coatings grown on 7075 Al alloy from silicate-based solution using plasma electrolytic oxidation. *Trans. Nonferrous Met. Soc. China* **2021**, *31*, 3659–3676. [CrossRef]
51. Li, R.; Li, T.; Zhou, Q. Impact of Titanium Dioxide (TiO_2) Modification on Its Application to Pollution Treatment-A Review. *Catalysts* **2020**, *10*, 804. [CrossRef]
52. Li, S.; Li, Y.; Shao, L.; Wang, C. Direct Z-scheme N-doped TiO_2/MoS_2 Heterojunction Photocatalyst for Photodegradation of Methylene Blue under Simulated Sunlight. *Chemistryselect* **2021**, *6*, 181–186. [CrossRef]
53. Xu, T.; Wang, M.; Wang, T. Effects of N Doping on the Microstructures and Optical Properties of TiO_2. *J. Wuhan Univ. Technol. -Mater. Sci. Ed.* **2019**, *34*, 55–63. [CrossRef]
54. Ma, X.; Zhang, Z.; Tian, J.; Xu, B.; Ping, Q.; Wang, B. Hierarchical TiO_2/C micro-nano spheres as high-performance anode materials for sodium ion batteries. *Funct. Mater. Lett.* **2018**, *11*, 1850021. [CrossRef]
55. Erdal, M.O.; Kocyigit, A.; Yildirim, M. The C-V characteristics of TiO_2/p-Si/Ag, GNR doped TiO_2/p-Si/Ag and MWCNT doped TiO_2/p-Si/Ag heterojunction devices. *Chin. J. Phys.* **2020**, *64*, 163–173. [CrossRef]
56. Luo, X.Y.; Huang, R.Y.; Zhao, D.F.; Zhu, T.; Deng, J.M. Preparation and photocatalytic performance of silver-modified and nitrogen-doped TiO_2 nanomaterials with oxygen vacancies. *New J. Chem.* **2021**, *45*, 4694–4704.
57. Zhu, X.D.; Xu, H.Y.; Yao, Y.; Liu, H.; Wang, J.; Feng, W.; Chen, S.H. Effects of Ag^0-modification and Fe^{3+}-doping on the structural, optical and photocatalytic properties of TiO_2. *Rsc Adv.* **2019**, *9*, 40003–40012. [CrossRef]
58. Zheng, X.; Zhang, D.; Gao, Y.; Wu, Y.; Liu, Q.; Zhu, X. Synthesis and characterization of cubic Ag/TiO_2 nanocomposites for the photocatalytic degradation of methyl orange in aqueous solutions. *Inorg. Chem. Commun.* **2019**, *110*, 107589. [CrossRef]

59. Wu, J.; Ma, X.; Xu, L.; Zhao, B.; Chen, F. Fluorination promoted photoinduced modulation of Pt clusters on oxygen vacancy enriched TiO_2/Pt photocatalyst for superior photocatalytic performance. *Appl. Surf. Sci.* **2019**, *489*, 510–518. [CrossRef]
60. Bharti, A.; Cheruvally, G. V-doped TiO_2 supported Pt as a promising oxygen reduction reaction catalyst: Synthesis, characterization and in-situ evaluation in proton exchange membrane fuel cell. *J. Power Sources* **2017**, *363*, 413–421. [CrossRef]
61. Marinho, B.A.; Djellabi, R.; Cristovao, R.O.; Loureiro, J.M.; Boaventura, R.A.R.; Dias, M.M.; Lopes, J.C.B.; Vilar, V.J.P. Intensification of heterogeneous TiO_2 photocatalysis using an innovative micro-meso-structured-reactor for Cr(VI) reduction under simulated solar light. *Chem. Eng. J.* **2017**, *318*, 76–88. [CrossRef]
62. Zhang, S.; Cao, X.; Wu, J.; Zhu, L.; Gu, L. Preparation of hierarchical CuO@TiO_2 nanowire film and its application in photoelectrochemical water splitting. *Trans. Nonferrous Met. Soc. China* **2016**, *26*, 2094–2101. [CrossRef]
63. Sha, M.A.; Meenu, P.C.; Sumi, V.S.; Bhagya, T.C.; Sreelekshmy, B.R.; Shibli, S.M.A. Tuning of electron transfer by Ni-P decoration on CeO_2-TiO_2 heterojunction for enhancement in photocatalytic hydrogen generation. *Mater. Sci. Semicond. Processing* **2020**, *105*, 104742.
64. Prabakaran, S.; Nisha, K.D.; Harish, S.; Archana, J.; Navaneethan, M.; Ponnusamy, S.; Muthamizhchelvan, C. Synergistic effect and enhanced electrical properties of TiO_2/SnO_2/ZnO nanostructures as electron extraction layer for solar cell application. *Appl. Surf. Sci.* **2019**, *498*, 143702. [CrossRef]
65. Chang, J.; Zhang, Q.; Liu, Y.; Shi, Y.; Qin, Z. Preparation of Fe_3O_4/TiO_2 magnetic photocatalyst for photocatalytic degradation of phenol. *J. Mater. Sci.-Mater. Electron.* **2018**, *29*, 8258–8266. [CrossRef]
66. Ponnusamy, G.; Francis, L.; Loganathan, K.; Ogunbiyi, O.O.; Jasim, S.; Sathrhasivam, J. Removal of cyanotoxins in drinking water using ozone and ozone-hydrogen peroxide (peroxone). *J. Water Supply Res. Technol.-Aqua* **2019**, *68*, 655–665. [CrossRef]
67. Ding, W.; Jin, W.; Cao, S.; Zhou, X.; Wang, C.; Jiang, Q.; Huang, H.; Tu, R.; Han, S.; Wang, Q. Ozone disinfection of chlorine-resistant bacteria in drinking water. *Water Res.* **2019**, *160*, 339–349. [CrossRef]
68. Guan, X.; Ma, Z.; Li, Z.; Zhu, Y.; You, H. Study on the Floating Bed Ozone Catalytic Oxidation System for Printing and DyeingWastewater Advanced Treatment. *Technol. Water Treat.* **2018**, *44*, 80–83.
69. Zhang, Y.; Zang, T.; Yan, B.; Wei, C. Distribution Characteristics of Volatile Organic Compounds and Contribution to Ozone Formation in a Coking Wastewater Treatment Plant. *Int. J. Environ. Res. Public Health* **2020**, *17*, 553. [CrossRef]
70. Liu, M.; Preis, S.; Kornev, L.; Hu, Y.; Wei, C. Pulsed corona discharge for improving treatability of coking wastewater. *J. Environ. Sci.* **2018**, *64*, 306–316. [CrossRef]
71. He, C.; Wang, J.; Xu, H.; Ji, X.; Wang, W.; Xu, X. Treatment of Bio-Treated Coking Wastewater by Catalytic Ozonation with Semi-Batch and Continuous Flow Reactors. *Water* **2020**, *12*, 2532. [CrossRef]
72. Wright, A.; Marsh, A.; Ricciotti, F.; Shaw, A.; Iza, F.; Holdich, R.; Bandulasena, H. Microbubble-enhanced dielectric barrier discharge pretreatment of microcrystalline cellulose. *Biomass Bioenergy* **2018**, *118*, 46–54. [CrossRef] [PubMed]
73. Zhang, F.; Yang, H.; Gui, X.; Schonherr, H.; Kappl, M.; Cao, Y.; Xing, Y. Recent advances for understanding the role of nanobubbles in particles folation. *Adv. Colloid Interface Sci.* **2021**, *291*, 102403. [CrossRef] [PubMed]
74. Temesgen, T.; Bui, T.T.; Han, M.; Kim, T.L.; Park, H. Micro and nanobubbles technologies as a new horizon for water-treatment techniques: A review. *Adv. Colloid Interface Sci.* **2017**, *246*, 40–51. [CrossRef] [PubMed]
75. Seridou, P.; Kalogerakis, N. Disinfection applications of ozone micro- and nanobubbles. *Environ. Sci.-Nano* **2021**, *8*, 3493–3510. [CrossRef]
76. Duan, L.; Yang, L.; Jin, J.; Yang, F.; Liu, D.; Hu, K.; Wang, Q.; Yue, Y.; Gu, N. Micro/nano-bubble-assisted ultrasound to enhance the EPR effect and potential theranostic applications. *Theranostics* **2020**, *10*, 462–483. [CrossRef] [PubMed]
77. Li, H.Z.; Hu, L.M.; Xia, Z.R. Impact of Groundwater Salinity on Bioremediation Enhanced by Micro-Nano Bubbles. *Materials* **2013**, *6*, 3676–3687. [CrossRef]
78. Takahashi, M.; Kawamura, T.; Yamamoto, Y.; Ohnari, H.; Himuro, S.; Shakutsui, H. Effect of Shrinking Microbubble on Gas Hydrate Formation. *J. Phys. Chem. B* **2003**, *10*, 2171–2173. [CrossRef]
79. Zhang, H.; Guo, Z.; Zhang, X. Surface enrichment of ions leads to the stability of bulk nanobubbles. *Soft Matter* **2020**, *16*, 5470–5477. [CrossRef]
80. Sun, L.; Zhang, F.; Guo, X.; Qiao, Z.; Zhu, Y.; Jin, N.; Cui, Y.; Yang, W. Research progress on bulk nanobubbles. *Particuology* **2022**, *60*, 99–106. [CrossRef]
81. Takahashi, M.; Ishikawa, H.; Asano, T.; Horibe, H. Effect of Microbubbles on Ozonized Water for Photoresist Removal. *J. Phys. Chem. C* **2012**, *116*, 12578–12583. [CrossRef]
82. Koda, Y.; Miyazaki, T.; Sato, E.; Horibe, H. Oxidative Decomposition of Organic Compounds by Ozone Microbubbles in Water. *J. Photopolym. Sci. Technol.* **2019**, *32*, 615–618. [CrossRef]
83. Jothinathan, L.; Cai, Q.Q.; Ong, S.L.; Hu, J.Y. Fe-Mn doped powdered activated carbon pellet as ozone catalyst for cost-effective phenolic wastewater treatment: Mechanism studies and phenol by-products elimination. *J. Hazard. Mater.* **2022**, *424*, 127483. [CrossRef]
84. Yang, H.; Ma, W.; Jiang, X.; Wu, J.; Zhang, L.; Hu, J. Pilot Study on Optimization of Ozone Catalytic Oxidation Process and Its Equipment. *China Water Wastewater* **2021**, *37*, 89–93.
85. Li, H.; Yi, F.; Li, X.; Gao, X. Numerical modeling of mass transfer processes coupling with reaction for the design of the ozone oxidation treatment of wastewater. *Front. Chem. Sci. Eng.* **2021**, *15*, 602–614. [CrossRef]

86. Bustos-Terrones, Y.; Rangel-Peraza, J.G.; Sanhouse, A.; Bandala, E.R.; Torres, L.G. Degradation of organic matter from wastewater using advanced primary treatment by O_3 and O_3/UV in a pilot plant. *Phys. Chem. Earth* **2016**, *91*, 61–67. [CrossRef]
87. Wang, B.; Shi, W.; Zhang, H.; Ren, H.Y.; Xiong, M.Y. Promoting the ozone-liquid mass transfer through external physical fields and their applications in wastewater treatment: A review. *J. Environ. Chem. Eng.* **2021**, *9*, 106115. [CrossRef]
88. Qin, Y.; Jiao, W.; Yang, P.; Liu, Y. Research Progress of Enhancement of Ozone Mass Transfer. *Chin. J. Process Eng.* **2017**, *17*, 420–426.
89. Jiao, W.; Qin, Y.; Wang, Y.; Guo, L.; Liu, Y. Enhancement performance of ozone mass transfer by high gravity technology. *Desalination Water Treat.* **2017**, *66*, 195–202. [CrossRef]
90. Matsumoto, M.; Wada, Y.; Xu, K.; Onoe, K.; Hiaki, T. Enhanced generation of active oxygen species induced by O_3 fine bubble formation and its application to organic compound degradation. *Environ. Technol.* **2021**, *28*, 1–9. [CrossRef]
91. Assadi, A.A.; Bouzaza, A.M.; Merabet, S.; Wolbert, D. Modeling and simulation of VOCs removal by nonthermal plasma discharge with photocatalysis in a continuous reactor: Synergetic effect and mass transfer. *Chem. Eng. J.* **2014**, *258*, 119–127. [CrossRef]
92. Patel, S.; Agarwal, R.; Majumder, S.K.; Das, P.; Ghosh, P. Kinetics of ozonation and mass transfer of pharmaceuticals degraded by ozone fine bubbles in a plant prototype. *Heat Mass Transf.* **2020**, *56*, 385–397. [CrossRef]
93. Sun, Z.; Wang, Y.; Chen, X.; Zhu, N.; Yuan, H.; Lou, Z. Variation of dissolved organic matter during excess sludge reduction in microbubble ozonation system. *Environ. Sci. Pollut. Res.* **2021**, *28*, 6090–6098. [CrossRef]
94. Cheng, W.; Jiang, L.; Quan, X.; Cheng, C.; Huang, X.; Cheng, Z.; Yang, L. Ozonation process intensification of p-nitrophenol by in situ separation of hydroxyl radical scavengers and microbubbles. *Water Sci. Technol.* **2019**, *80*, 25–36. [CrossRef] [PubMed]
95. Tsujimoto, K.; Horibe, H. Effect of pH on Decomposition of Organic Compounds Using Ozone Microbubble Water. *J. Photopolym. Sci. Technol.* **2021**, *34*, 485–489. [CrossRef]
96. Takahashi, M.; Shirai, Y.; Sugawa, S. Free-Radical Generation from Bulk Nanobubbles in Aqueous Electrolyte Solutions: ESR Spin-Trap Observation of Microbubble-Treated Water. *Langmuir* **2021**, *37*, 5005–5011. [CrossRef] [PubMed]
97. Coey, J.M.D.; Moebius, M.; Gillen, A.J.; Sen, S. Generation and stability of freestanding aqueous microbubbles. *Electrochem. Commun.* **2017**, *76*, 38–41. [CrossRef]
98. Li, P.; Takahashi, M.; Chiba, K. Degradation of phenol by the collapse of microbubbles. *Chemosphere* **2009**, *75*, 1371–1375. [CrossRef]
99. Jin, J.; Wang, R.; Tang, J.; Yang, L.; Feng, Z.; Xu, C.; Yang, F.; Gu, N. Dynamic tracking of bulk nanobubbles from microbubbles shrinkage to collapse. *Colloids Surf. A-Physicochem. Eng. Asp.* **2020**, *589*, 124430. [CrossRef]
100. Meng, F.; Zhu, B.; Zhou, F.; Zeng, Y.; Han, J.; Yang, J.; Zhang, S.; Zhong, Q. Mechanism study on TiO_2 inducing $\cdot O_2^-$ and O·H radicals in O_3/H_2O_2 system for high-efficiency NO oxidation. *J. Hazard. Mater.* **2020**, *399*, 123033. [CrossRef] [PubMed]
101. Liu, Z.; Chys, M.; Yang, Y.; Demeestere, K.; Van Hulle, S. Oxidation of Trace Organic Contaminants (TrOCs) in Wastewater Effluent with Different Ozone-Based AOPs: Comparison of Ozone Exposure and ·OH Formation. *Ind. Eng. Chem. Res.* **2019**, *58*, 8896–8902. [CrossRef]
102. Kim, T.-K.; Kim, T.; Lee, I.; Cjoi, K.; Zoh, K.-D. Removal of tetramethylammonium hydroxide (TMAH) in semiconductor wastewater using the nano-ozone H_2O_2 process. *J. Hazard. Mater.* **2021**, *409*, 123759. [CrossRef]
103. Shangguan, Y.; Yu, S.; Gong, C.; Wang, Y.; Yang, W.; Hou, L. A review of microbubble and its applications in ozonation. *IOP Conf.* **2018**, *128*, 012149. [CrossRef]
104. Guo, Z.; Wang, X.; Zhang, X. Stability of Surface Nanobubbles without Contact Line Pinning. *Langmuir* **2019**, *35*, 8482–8489. [CrossRef] [PubMed]
105. Olszok, V.; Rivas-Botero, J.; Wollmann, A.; Benker, B.; Weber, A.P. Particle-induced nanobubble generation for material-selective nanoparticle flotation. *Colloids Surf. A-Physicochem. Eng. Asp.* **2020**, *592*, 124576. [CrossRef]
106. Fan, W.; Zhou, Z.; Wang, W.; Huo, M.; Zhang, L.; Zhu, S.; Yang, W.; Wang, X. Environmentally friendly approach for advanced treatment of municipal secondary effluent by integration of micro-nano bubbles and photocatalysis. *J. Clean. Prod.* **2019**, *237*, 117828. [CrossRef]
107. Atkinson, A.J.; Apul, O.G.; Schneider, O.; Garcia-Segura, S.; Westerhoff, P. Nanobubble Technologies Offer Opportunities to Improve Water Treatment. *Acc. Chem. Res.* **2019**, *52*, 1196–1205. [CrossRef] [PubMed]
108. Yasui, K.; Tuziuti, T.; Kanematsu, W. High temperature and pressure inside a dissolving oxygen nanobubble. *Ultrason. Sonochemistry* **2019**, *55*, 308–312. [CrossRef] [PubMed]
109. Zhang, X.Y.; Wang, Q.S.; Wu, Z.X.; Tao, D.P. An experimental study on size distribution and zeta potential of bulk cavitation nanobubbles. *Int. J. Miner. Metall. Mater.* **2020**, *27*, 152–161. [CrossRef]
110. Zhang, M.M.; Seddon, J.R.T. Nanobubble-Nanoparticle Interactions in Bulk Solutions. *Langmuir* **2016**, *32*, 11280–11286. [CrossRef]
111. Nirmalkar, N.; Pacek, A.W.; Barigou, M. Interpreting the interfacial and colloidal stability of bulk nanobubbles. *Soft Matter* **2018**, *14*, 9643–9656. [CrossRef] [PubMed]
112. Perez Sirkin, Y.A.; Gadea, E.D.; Scherlis, D.A.; Molinero, V. Mechanisms of Nucleation and Stationary States of Electrochemically Generated Nanobubbles. *J. Am. Chem. Soc.* **2019**, *141*, 10801–10811. [CrossRef]
113. Li, Q.; Ying, Y.L.; Liu, S.C.; Hu, Y.X.; Long, Y.T. Measuring temperature effects on nanobubble nucleation via a solid-state nanopore. *Analyst* **2020**, *145*, 2510–2514. [CrossRef] [PubMed]
114. German, S.R.; Edwards, M.A.; Chen, Q.; White, H.S. Laplace Pressure of Individual H_2 Nanobubbles from Pressure-Addition Electrochemistry. *Nano Lett.* **2016**, *16*, 6691–6694. [CrossRef] [PubMed]

115. Xiao, W.; Wang, X.; Zhou, L.; Zhou, W.; Wang, J.; Qin, W.; Qiu, G.; Hu, J. Influence of Mixing and Nanosolids on the Formation of Nanobubbles. *J. Phys. Chem. B* **2019**, *123*, 317–323. [CrossRef]
116. Yasui, K.; Tuziuti, T.; Kanematsu, W. Mysteries of bulk nanobubbles (ultrafine bubbles); stability and radical formation. *Ultrason. Sonochem.* **2018**, *48*, 259–266. [CrossRef]
117. Levanov, A.V.; Isaikina, O.Y.; Gasanova, R.B.; Lunin, V.V. Solubility of Ozone and Kinetics of Its Decomposition in Aqueous Chloride Solutions. *Ind. Eng. Chem. Res.* **2018**, *57*, 14355–14364. [CrossRef]
118. Yao, K.; Chi, Y.; Fei, W.; Yan, J.; Ni, M.; Cen, K. The effect of microbubbles on gas-liquid mass transfer coefficient and degradation rate of COD in wastewater treatment. *Water Sci. Technol.* **2016**, *73*, 1969–1977. [CrossRef] [PubMed]
119. Zhang, J.; Qian, Z.; Liu, C.; Guo, Y.; Liu, M.; Wang, X. Performance and mechanism of catalytic microbubble ozonation of acid red 3R. *Chin. J. Environ. Eng.* **2021**, *15*, 1199–1208.
120. Zepeng, Q. *Characteristics of Synergistic Treatment of Acid Red 3R Wasterwater using Microbubble-Ozone-Catalyst System*; Hebei University of Science and Technology: Shijiazhuang, China, 2020.
121. Sun, F.; Liu, H.; Chu, Z.; Zhai, P.; Chen, T.; Wang, H.; Zou, X.; Chen, D. The effect of isomorphic substitution on siderite activation of hydrogen peroxide: The decomposition of H_2O_2 and the yield of center dot OH. *Chem. Geol.* **2021**, *585*, 120555. [CrossRef]
122. Hussain, H.; Tocci, G.; Woolcot, T.; Torrelles, X.; Pang, C.L.; Humphrey, D.S.; Yim, C.M.; Grinter, D.C.; Cabailh, G.; Bikondoa, O.; et al. Structure of a model TiO_2 photocatalytic interface. *Nat. Mater.* **2017**, *16*, 461–466. [CrossRef]